Electronic properties and chemical trends of the arsenic *in situ* impurities in $Hg_{1-x}Cd_xTe$: First-principles study

L. Z. Sun,[1,2,*] Xiaoshuang Chen,[2,†] Jijun Zhao,[3] J. B. Wang,[1] Y. C. Zhou,[1] and Wei Lu[2,‡]

[1]*Key Laboratory of Low Dimensional Materials & Application Technology, Ministry of Education, Institute of Modern Physics, Xiangtan University, Xiangtan 411105, China*

[2]*National Laboratory for Infrared Physics, Shanghai Institute of Technical Physics, Chinese Academy of Sciences, 200083 Shanghai, China*

[3]*State Key Laboratory of Materials Modification by Laser, Electron, and Ion Beams, School of Physics and Optoelectronic Technology and College of Advanced Science and Technology, Dalian University of Technology, Dalian 116024, China*

(Received 30 October 2006; revised manuscript received 14 February 2007; published 23 July 2007)

The structural and electronic properties of the arsenic *in situ* impurity in $Hg_{1-x}Cd_xTe$ (MCT) have been studied by combining the full-potential linear augmented plane wave and plane-wave pseudopotential methods based on the density functional theory. The structural relaxations, the local charge density, and the densities of states were computed to investigate the impurity effects on the electronic structure. The bonding characteristic between the impurity and the host atoms was discussed by analyzing the valence and the bonding charge density. The defect levels introduced by the *in situ* arsenic impurity were determined by the transition energy levels which agree well with the experimental results. Based on the calculated formation energy, the chemical trends of the *in situ* arsenic impurity and the compensation effects between As_{Te} and As_{Hg} in $Hg_{1-x}Cd_xTe$ have been studied systematically. A brief discussion on the activation model of the postgrowth annealing process of arsenic-doped MCT was also presented.

DOI: 10.1103/PhysRevB.76.045219 PACS number(s): 61.72.Bb, 61.72.Vv, 71.55.Gs

I. INTRODUCTION

One of the most important limitations of the applied prospect for the semiconductor materials is the difficulty of *n*- or *p*-type doping via incorporation of suitable impurities. For example, ZnSe materials can be fabricated as blue emitting laser diodes, which is mainly profit from the achievement of sufficient *p*-type doping.[1,2] Another typical instance is ZnO. The difficulty of efficient *p*-type doping[3] is the limitation for its practical applications until now. In general, the doping controllability is the major challenge in most semiconductors. The difficulties, generally speaking, concern two aspects: dopant stability and doping efficiency. The dopant stability, consequently low diffusivity, mainly determines the performance of homo- or heterojunction devices which rely on the sharpness of the doping profile.[4] The problem of the doping efficiency might arise from a variety of causes. Firstly, an element can be a desirable dopant in certain semiconductor, depending on whether it can produce a shallow impurity level. The shallow impurity levels can provide high thermal excitation of carriers into the valence or conduction bands, namely, it can easily be electronically activated. Secondly, the solubility of the dopant in a host lattice can be a source of doping restrict. Lastly, the compensation effect is another most important obstacle to be overcome in the doping process. The compensation can either result from the intrinsic defects with low formation energy or from the dopant-induced *AX* (*DX*) centers.[5–8] As for the amphoteric dopant, the self-compensation is a crucial limitation of the doping efficiency, such as the doping behavior of arsenic in II-VI semiconductors and alloys. The experimental results have indicated that arsenic can provide a shallow acceptor level in $Hg_{1-x}Cd_xTe$ (MCT) grown by bulk method,[9] liquid phase epitaxy (LPE),[10] molecular beam epitaxy (MBE),[11–13] and metal organic chemical vapor deposition.[14] At the same time, the amphoteric behavior of arsenic in HgCdTe has been found. Arsenic behaves as a *p*-type dopant under Hg-rich growth conditions and behaves as an *n*-type or unactive dopant under Te-rich growth conditions.[9,10,13,14] Moreover, the theoretical and experimental results[15–18] showed that there is a significant fraction of arsenic residing on the cation sublattice even under cation-saturated growth conditions. So, an annealing process is required for its electric activation.[19] However, as the doping levels reach 5×10^{18} cm^{-3}, the active efficiency of the *p*-type arsenic doping drastically drops due to the strong self-compensation effect.[20,21] So, the amphoteric behavior of the arsenic *in situ* impurities in MCT is a typical prototype to systematically study the self-compensating effect.

The purpose of this paper is to identify the amphoteric doping behavior of arsenic in MCT. MCT is currently one of the most widely used infrared materials since its band gap can be tuned by varying the alloy composition to scope the infrared air windows. Due to the low diffusivity of the group V elements in MCT (Ref. 15) compared with the native acceptor and the group I elements, attention has focused on the group V elements for decades, especially arsenic, as the *p*-type dopant in heterojunction devices. Although a simple model of the arsenic amphoteric behavior has been suggested, there is no comprehensive consensus on the microscopic mechanism of group V impurity incorporation in MCT. Moreover, the alloying effect of MCT interferes with the behavior of the amphoteric dopant, which makes the study more complicated. It is affirmable that the understanding of the amphoteric behavior of As in MCT is essentially important for qualifying the material growth and device design. In a previous work,[22] we reported the relaxations, bonding mechanism, and the electronic structure of As_{Hg} in

 ©2007 The American Physical Society

$Hg_{0.5}Cd_{0.5}Te$. In order to gain full understanding of the electronic behaviors and the compensation effect of the *in situ* As impurities in MCT, we have performed the total energy calculations of full-potential linear augmented plane wave (FP-LAPW) to systematically investigate the effect of the arsenic *in situ* impurity on the electronic structure, bonding mechanism between the impurity and the host atoms, the relaxation, and the chemical trends of the As *in situ* impurity in $Hg_{1-x}Cd_xTe$. In this paper, we choose $Hg_{0.5}Cd_{0.5}Te$ as the major prototype system. Furthermore, the results and conclusions of the calculations on $Hg_{0.5}Cd_{0.5}Te$ are confirmed and also extended to the other mole fractions by using plane-wave pseudopotential calculations with larger supercells. Our general understanding of the amphoteric impurity behaviors and its self-compensating effect in MCT from the present study is expected to be applicable also to other semiconductors and alloys.

The remainder of the paper is organized as follows. Section II describes our computational methods. The results and discussions are presented in Sec. III. We discuss the relaxation procedure corresponding to different mole fractions, the bonding mechanism between the impurity and host atoms, and the impurity levels. The relationship between formation energy and the mole fractions of MCT, and the compensation effect between As_{Hg} and As_{Te} are systematically discussed. Section IV gives a brief summary of this work.

II. COMPUTATIONAL PROCEDURE

The density functional theory[23] calculations were performed using the FP-LAPW method implemented in the WIEN2K package.[24] We adopt Perdew-Burke-Ernzerhof functional[25] to describe the exchange-correlation interaction. We consider a $2\times2\times2$ supercell (SC) with a total of 64 atoms, consisting of eight quasi-zinc-blende crystal structure of the unit cells of $Hg_{1-x}Cd_xTe$ (each unit cell contains eight atoms including four Te atoms and four cations of Hg and Cd atoms corresponding to the fraction x). The doped system was modeled by putting one As atom at the center of a periodic supercell. A $2\times2\times1$ supercell with 32 atoms without any impurity was chosen as a reference system for comparison purpose, and the computational parameters are set to be the same as the As doping cases. To ensure convergence well, the muffin-tin (MT) radii and the number of k points for generating the final results have been carefully chosen after optimization. 8 and 32 k points in the irreducible Brillouin zone have been chosen for doped and pure MCT, respectively. A satisfactory self-consistent convergence has been achieved by considering a number of FP-LAPW basis functions up to $R_{MT}K_{\max}=6.0$ for the 64-atom supercell and $R_{MT}K_{\max}=7.0$ for 32-atom supercell. $K_{\max}$ is the maximum value of the plane-wave vector which determines the energy cutoff for the plane-wave expansion. Self-consistent iteration was considered to be converged when both the total energy and the total charge in the atomic sphere are stable within 10^{-4} eV per unit cell and 10^{-4} electron charges per atom, respectively. The relaxation procedures were conducted following the damped Newton dynamics schemes.[26,27] The criterion of the force convergence for all atoms was 0.05 eV/Å. The relativistic effect of spin-orbit (SO) coupling was also included.

To confirm the results from the 64-atoms supercell using FP-LAPW calculations and to extend the conclusions to the other mole fractions of MCT, plane-wave pseudopotential calculations were performed using the Vienna *ab initio* simulation package (VASP).[28,29] In the VASP calculations, the core-electron interaction was modeled by the ultrasoft pseudopotentials,[30] which can yield reasonably precise results with relatively low cutoff energy. Thus, it is possible to deal with the larger supercell. In this work, supercells with 256 and 512 atoms have been chosen. The plane-wave cutoff energy was chosen as 300 eV, and the Brillouin zone was sampled by using $5\times5\times5$ and $3\times3\times3$ Gamma centered Monkhorst-Pack grids for 256- and 512-atom supercells, respectively. The energy convergent criterion was 1×10^{-4} eV per unit cell, and forces on all relaxed atoms were less than 0.01 eV/Å.

It is well known that local density approximation calculations typically underestimate the band gap of a semiconductor and are unable to give the absolute positions of the impurity level accurately. Here, we emphasize on the analysis of the defect formation energy and the transition energy levels.[7,31] At temperature of 0 K, the formation energy of arsenic impurity in a given charge state q in MCT is given by

$$\Delta H_f(As_\alpha,q) = E(As_\alpha,q) + E(\alpha) - E(\mathrm{MCT}) - E(As) + qE_{VBM} + qE_F + \mu_\alpha - \mu_{As}. \quad (1)$$

$\Delta H_f(As_\alpha,q)$ is the formation energy for a supercell containing the arsenic dopant in charge state q. $E(As_\alpha,q)$ and $E(\mathrm{MCT})$ are the total energies for the supercell containing the arsenic dopant in charge state q and for the supercell of the same size without impurity, respectively. $E(\alpha)$ and $E(As)$ are the total energies of host atoms (Te, Cd, and Hg) and the impurity arsenic atom, respectively. The atomic chemical reservoir is Te_2 molecule, Cd and Hg gas for host atoms, and As_4 molecule for arsenic impurity, respectively, which coincide with the MBE growth conditions. μ_α and μ_{As} are the external chemical potentials of the host atoms and the arsenic impurity, respectively. Equation (1) indicates that the formation energy with arsenic dopant, $\Delta H_f(As_\alpha,q)$, is a function of the E_F and the chemical potential of host and arsenic impurity, μ_α and μ_{As}. The defect transition energy level $\varepsilon_\alpha(q/q')$ is the Fermi energy E_F in Eq. (1), at which the formation energy $\Delta H_f(As_\alpha,q)$ of arsenic impurity with charge q is equal to that of another charge q'. The formation energy and transition energy levels of MCT with arsenic dopant were calculated by the projector-augmented wave (PAW) method for the 64-atom supercell. For the charged systems with impurity, a uniform background charge is added to keep the global charge of the periodic supercell neutral. The total energy of the systems with charged defect has been corrected for the interaction of the charged defect with the compensating background and its periodic images.[32] For the 64-atom SC, the error bar is about 0.2 and 0.1 eV for the calculated formation energy and transition energy level, respectively, due to the finite cell size and basis set.

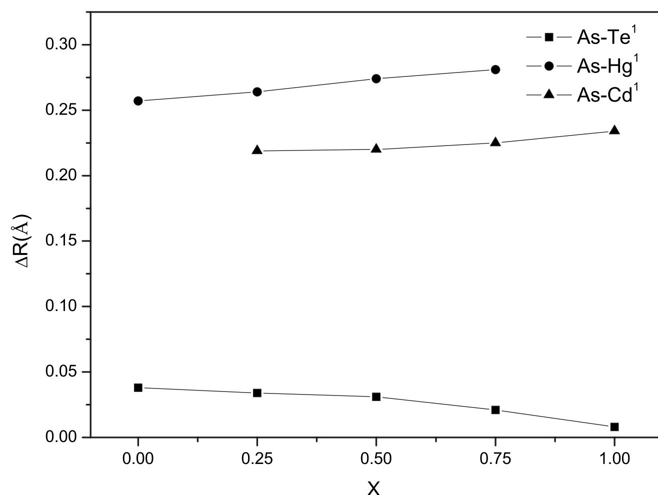

FIG. 1. Relationship between the inward radial relaxations of the NN atoms and the mole fraction of MCT.

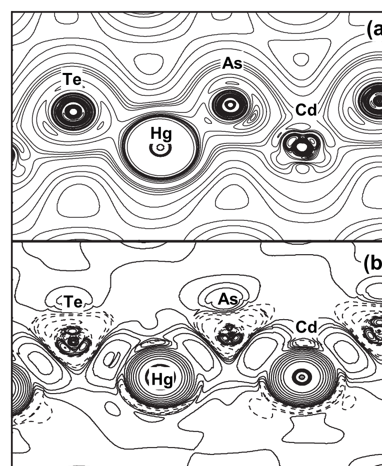

FIG. 2. Valence charge density and bonding charge density in the (110) plane for As_{Te}. The contour step size is $1\times10^{-3}e/a.u.^3$ and $0.5\times10^{-3}e/a.u.^3$ for total charge density and bonding charge density, respectively.

III. RESULTS AND DISCUSSIONS

A. Structural relaxation

The existence of the *in situ* arsenic impurity in MCT induces the structural relaxation of the host atoms and modifies the electronic structure of the system. All the internal structural parameters of the supercell in this work were optimized by minimizing the total energy and quantum mechanical forces. Geometry optimizations reveal that the As impurity, either substituting Te or Hg (Cd atom for CdTe), leads to inward relaxations of the nearest-neighbor (NN) host atoms around the impurity. The radial relaxations of the NN atoms around the impurity calculated by using the PAW method for 64-atom supercell are shown in Fig. 1. On the one hand, the inward radial relaxations derive from the difference of the covalent radii between the As and the host atoms substituted (the covalent radii are 1.20, 1.36, 1.49, and 1.48 for As, Te, Hg, and Cd, respectively). On the other hand, the inward relaxations of the NN atoms around impurity are induced by the strong bonding mechanism between the As and the host atoms. The detail will be discussed below. The results also show that the As_{Te} impurity induces larger inward radial relaxations of the NN atoms than As_{Hg}. The relaxations of the NN atoms around the impurity calculated by using the FP-LAPW method give the same inward relaxed trend. However, the inward radial relaxations of the NN atoms derived from the PAW method are nearly three times larger than those from the FP-LAPW method. For example, as $x=0.5$ for the As_{Hg} case, the inward radial relaxations of NN Te is 0.01 Å (Ref. 22) and 0.03 Å for the FP-LAPW and the PAW method, respectively. Larger radial relaxation of the PAW calculations mainly comes from relatively small force criterion by comparison with that of FP-LAPW calculations. Considering the large computational time consuming, full relaxation of atomic positions was used in PAW calculations, while symmetry constraint was applied in FP-LAPW calculations. To confirm the results of the FP-LAPW and PAW calculations on the 64-atom supercell, larger supercells with 256 and 512 atoms have been used. The structural relaxations are conducted by using the PAW method implemented in VASP. The results with 256- and 512-atom supercells give the same relaxation trend of NN atoms as that of the 64-atom SC. Approximately linear relationship between the radial inward relaxation of the NN atoms and the mole fractions of MCT is shown in Fig. 1. The inward relaxations of the NN atoms become smaller as the mole fraction becomes larger in the As_{Hg} doping cases, while in the As_{Te} doping cases the radial inward relaxations become larger as the mole fraction becomes larger.

B. Bonding mechanism

To find out the reason of the NN atom inward relaxation in MCT caused by the As impurity, the valence and the bonding charge density have been calculated. The bonding charge density is defined as the difference between the total charge density in the solid and the superpositions of neutral atomic charge densities placed at atomic sites, i.e.,

$$\Delta\rho(r) = \rho_{solid}(r) - \sum_{\alpha} \rho_{\alpha}(r - r_{\alpha}). \quad (2)$$

Therefore, the bonding charge density represents the net charge redistribution as atoms are brought together to form the crystal. The bond rehybridization induced by the As impurity can also be revealed clearly by the bonding charge density. The valence and the bonding charge density of $Hg_{0.5}Cd_{0.5}Te$ in the (110) plane for the As_{Te} were calculated by using the FP-LAPW method and are shown in the Fig. 2 (refer to Ref. 22 for the results of the As_{Hg} case). In the figures, the dash lines denote that the electrons move out relative to that of the atom superposition. In Fig. 2, the charge density distributions between the arsenic impurity and the NN host atoms show the covalent characteristic. The bonding characteristic between the impurity and the host atoms is similar to the situation in the case of As_{Hg}.[22] The valence charge density along the line of As-Hg/Cd bond in the case of As_{Te} is shown in Fig. 3 (refer to Ref. 22 for the results in the case of As_{Hg}). The results indicate that

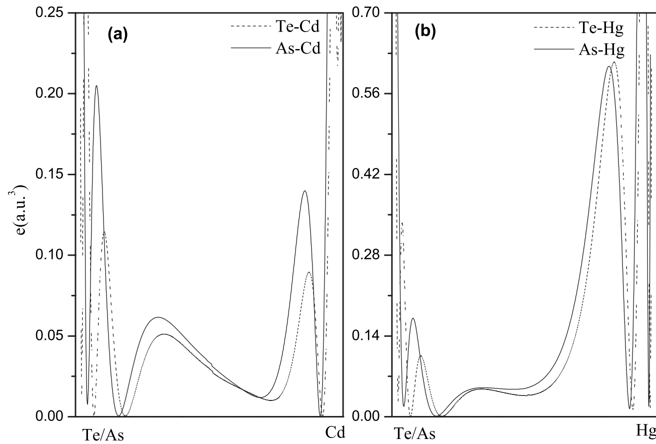

FIG. 3. Valence charge density along the bond line of As-Hg and As-Cd for the As_{Te} case and the total charge density along the bond line of Te-Hg and Te-Cd for the pure system.

As-Hg/Cd bonds for the As_{Te} case are covalent with stronger ionic characteristics than that of Te-Hg/Cd bond in the pure system. Together with the bonding mechanism analysis in the case of As_{Hg},[22] we can see that, in addition to the smaller arsenic radius, the strong bonding also results in the NN host atom inward relaxation. Moreover, the strong bonding characteristics account for the stably doping behavior of As in MCT, which produces low diffusivity of the As doping.

The total density of states (DOS) of As_{Te}-doped $Hg_{0.5}Cd_{0.5}Te$ is shown in Fig. 4. Substitution of a tellurium by an arsenic atom produces the resulting system metallic. Evidently, the Fermi level of the As_{Te}-doped system (see Ref. 22 for the discussions of the As_{Hg}) does not lie within the band gap which extends to the valence band, as shown in Fig. 4. The DOS integrated from the Fermi level to the midgap accommodates one electron. The results show that the impurity As_{Te} in MCT would behave as a single acceptor. The theoretical predications are in good agreement with the experimental results.[10,13] For the case of charged neutral As_{Te}, the defect center has a total of seven electrons. Two of

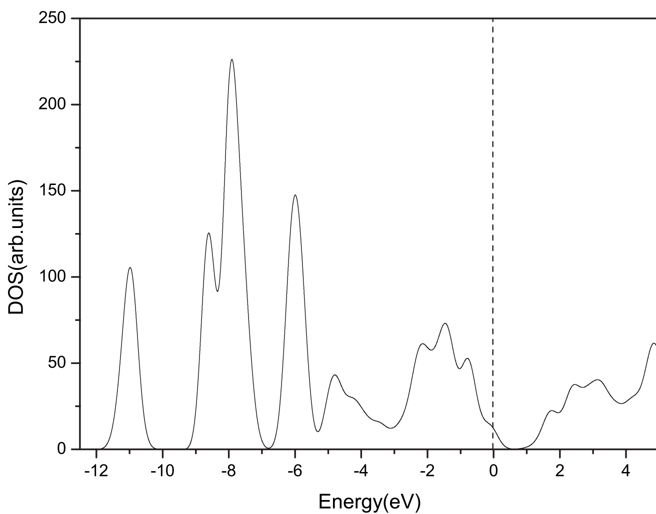

FIG. 4. Total DOS of As_{Te}-doped MCT-0.5. The Fermi level is set to zero.

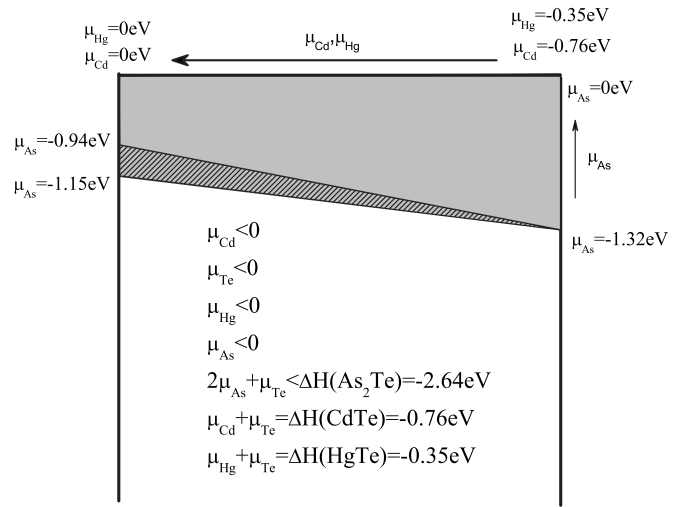

FIG. 5. Calculated available equilibrium chemical potential region for MCT:As in the two dimensional (μ_{Cd}, μ_{Hg}, and μ_{As}) plane. The shaded and diagonal area is forbidden under equilibrium growth condition.

them occupy the a_1^v states, five of them occupy the t_2^v states. One of unoccupied t_2^v state just above the valence band maximum (VBM) behaves as a single acceptor.

C. Formation energy

During the defect formation, there are particles exchanged between the host and the chemical reservoir. The defect formation energy depends sensitively on the atomic chemical potential, as well as on the Fermi energy, as indicated in Eq. (1). Moreover, there are some thermodynamic limits on the achievable values of the host and impurity atoms' chemical potentials. In order to maintain a stable MCT compound, to avoid precipitation of host and impurity element, and to avoid the formation of secondary phases between the dopant arsenic and host elements, the chemical potentials of Hg, Cd, Te, and As are limited as shown in Fig. 5. The analysis of bonding mechanism indicates that the As impurity forms strong bonds with the host atoms, which would easily produce secondary phases between arsenic and host elements. After thorough analysis, it shows that As forms stable compound As_2Te with Te. Comparing the MCT-0.5 with Te vacancy defect and the MCT-0.5 with double As interstitial impurities, the formation energy of As_2Te in MCT-0.5 crystal potential field was obtained to be about -2.64 eV. In present paper, we simply chose the formation energy of As_2Te in MCT-0.5 as the criterion for MCT. This treatment only affects the absolute values and do not influence the trend and the comparisons between the formation energies in the same mole fraction. The formation energy of As_2Te limits the chemical potential of As under the cation- or tellurium-rich conditions, as shown in Fig. 5. The shaded and shaded plus diagonal areas in the figure are forbidden under equilibrium growth condition for arsenic in CdTe and HgTe, which can be taken as the extreme situation of MCT. Above these chemical potential limits, secondary phase As_2Te will form. Under the cation-rich condition, the chemical potential

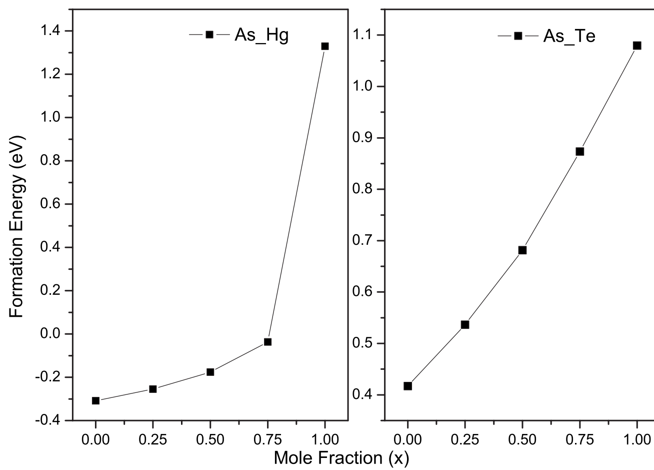

FIG. 6. Formation energy of As_{Te} and $As_{Hg/Cd}$ according to the mole fraction of MCT at the neutral charge state ($q=0$) and $\mu_i=0$.

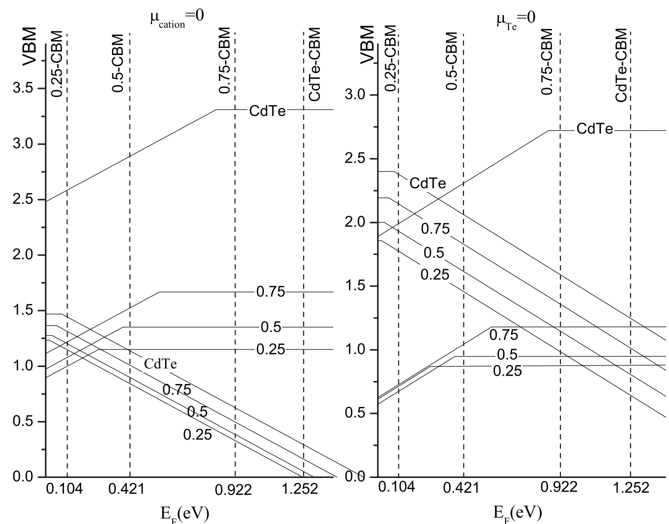

FIG. 7. Calculated formation energy of As_{Te} and $As_{Hg/Cd}$ according to the mole fraction of MCT as a function of the Fermi levels. The VBM of all the four mole fraction is set to zero.

of Te in MCT becomes complicated due to the alloying effects. In the present paper, we simply adopt the virtual crystal approximation (VCA) to predict the chemical potential of Te based on the formation energy of HgTe and CdTe (the formation energy of HgTe and CdTe is −0.35 and −0.76 eV, respectively). As pointed out in the previous work,[33] the VCA will introduce errors into the theoretical results of the formation energy. However, these errors would cancel with each other in the results by comparing between the formation energies, especially for the results of the dynamic levels.

The formation energies of the *in situ* As impurity in MCT for five different mole fractions ($x=0$, 0.25, 0.5, 0.75, and 1) under neutral charge state were calculated and shown in Fig. 6. In the figure, the chemical potential is $\mu_{cation}=0$ and $\mu_{Te}=0$ for As_{Hg} and As_{Te}, respectively. The results indicate that the formation energy for substituting Hg by As is much smaller than that of substituting Te for MCT. However, for CdTe, the formation energy of As_{Cd} is larger than that of As_{Te}. In this work, the formation energy of As_{Te} in CdTe is obtained as 1.01 eV, and this result agrees with the previous prediction.[7] The results shown in Fig. 6 indicate that the formation energy of As impurity in MCT has a nearly linear relationship with the mole fraction for both As_{Hg} and As_{Te} cases. The relationship denotes that the As doping can easily be accomplished as the mole fraction become smaller, which coincide with the experimental predictions.[34] It is worthy to mention that the linear relationship between the defect formation energy and mole fraction was also observed in mercury vacancy defect in MCT.[35] We predict that the occurrence of the linear relationship is due to the increased number of the weak Te-Hg bond with decreasing the mole fraction, which weakens the average bond strength of MCT.

It is known that whether an impurity can easily be incorporated in a material depends sensitively on the growth condition, such as the atomic chemical potential, the growth temperature, as well as the Fermi energy related to the doping levels. The dependence is especially important for the As dopant in MCT because it exhibits amphoteric behavior. In order to analyze the chemical trend of the As impurity in MCT, the formation energy as function of atomic chemical potential and Fermi energy has been calculated. Figure 7 shows the calculated formation energies of As-doped MCT for $x=0.25$, 0.5, 0.75, and 1 as a function of the Fermi energy under cation- and Te-rich growth conditions. The slope of the line gives the charge state of the doping at the Fermi energy. The transition energy level is the Fermi energy, at which the slope changes value. Under $\mu_{Te}=0$ condition, as shown in Fig. 7, the formation energy of As_{Hg} for $x=0.25$, 0.5, and 0.75 is smaller than that of As_{Te} as the Fermi energy shifts inside the band gap. These results indicate that the arsenic behaves as dominant *n*-type dopant for MCT as $x=0.25$, 0.5, and 0.75 under Te-rich condition. The experiments of MBE growth of HgCdTe (Refs. 20, 21, and 36) (for which the typical growth condition is Te saturated) and LPE growth of HgCdTe (Ref. 10) incorporate arsenic as dopant under Te-saturated condition, both resulting in *n*-type doping behavior. The results shown in Fig. 7 indicate that the formation energies of As_{Hg} are about 1.0–1.5 eV smaller than that of As_{Te} as the Fermi level at VBM. It indicates that As easily incorporates into the cation site under the Te-saturated growth condition, behaving as *n*-type dopant. However, under the Te-rich limit, the formation energy of As_{Cd} for CdTe is smaller than that of As_{Te} as E_F below 0.3 eV. As the Fermi energy shifts up toward the midgap, the formation energy of As_{Te} is smaller than that of As_{Cd}. Namely, the As_{Te} and As_{Cd} compensate each other at the Te-rich limit and the Fermi energy is pinned at a level closer to the VBM; consequently, the arsenic impurity in CdTe, even at Te-rich limit, tends to be slightly *p*-type dopant. Although there are few experimental reports under this extreme growth condition, arsenic-doped CdTe layers grown by organometallic vapor phase epitaxy produce *p*-type doping behavior even when the partial pressures of Cd and Te are equal.[37] Under $\mu_{Cd}=0$ condition, as shown in Fig. 7, the formation energy of As_{Te} is nearly 1 eV smaller than that of As_{Cd} for CdTe. The arsenic dominantly incorporates into the Te site, behaving as *p*-type dopant under the Cd-saturated condition. The result is in good agreement with the MBE growth CdTe doped by arsenic under Cd-saturated condition as efficient *p* type.[38] The differ-

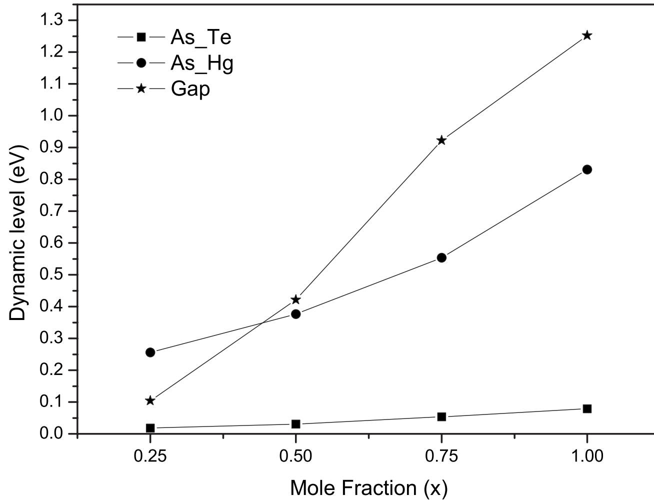

FIG. 8. Transition energy levels of As-doped MCT. The band gap is calculated in the present paper.

ence of the formation energy of As_{Hg} and As_{Te} for $x=0.25$, 0.5, and 0.75 is around 0.5 eV as the Fermi energy at VBM under Hg-rich limit. As for $x=0.25$, the formation energy of As_{Hg} is smaller than that of As_{Te} as the Fermi energy shifts inside the band gap. These results indicate that the arsenic in MCT-0.25 dominantly behaves as n-type dopant, even under Hg-saturated growth condition. The compensation effects between As_{Hg} and As_{Te} occur for $x=0.5$ and 0.75 and the Fermi energy is pinned at about 0.1 eV above VBM. Namely, arsenic doping in MCT-0.5 and MCT-0.75 tends to be slight p-type dopant under Hg-rich limit.

As shown in Fig. 7, the difference of the formation energy of As_{Hg} and As_{Te} is much smaller under Hg-rich limit than that under Te-rich limit. As mentioned above, with mole fraction around 0.25, the arsenic easily incorporates into the cation site, behaving as donor. In order to switch arsenic doping from n to p type, postgrowth annealing must be done. In the model developed by Berding *et al.*,[18] they suggested two steps in the annealing processes. In the first step, low Hg partial pressure is maintained to enhance the amount of metal vacancies (V_{Hg}) which aid transfers of atom. In the second step, saturated Hg partial pressure is maintained to fill the Hg vacancies. According to the calculated results in the present paper shown in Fig. 7, we argued that the second annealing step must be achieve under Hg-saturated condition mainly because the Hg-rich limit minimizes the difference of the formation energy between As_{Hg} and As_{Te}, which is beneficial for the arsenic transfer from the cation to the anion site achieving the p-type arsenic dopant activation.

The transition energy levels of As_{Hg} and As_{Te} for $x=0.25$, 0.5, and 0.75 and As_{Cd} and As_{Te} for CdTe have been calculated and shown in Fig. 8. The theoretical results show that the As_{Te} has shallow transition energy level $(0/-1)$ for all mole fractions of MCT. The transition energy levels become deeper as the mole fraction becomes larger. The trend of the transition energy level with regard to the variation of the mole fraction x agrees well with experiments.[39] The transition energy level $(0/-1)$ of CdTe is 78 meV, in good agreement with the experiments' ionization energy of arsenic-doped p-type CdTe [around 58–92 meV (Refs. 38 and 40)]. The transition energy level calculated for MCT-0.25 is 19 meV in the present paper, while the experimental data have shown that the ionization energy is about 6 meV (Ref. 20) for As_{Te} acceptor level for the mole fraction around 0.3. The calculated results reasonably agree with the experiment. The transition energy levels of As_{Hg} in MCT also move deeper as the mole fraction becomes larger. The results indicate that the impurity levels of As_{cation} tend to behave as deep center for CdTe and MCT with large mole fraction.

To briefly summarize, the calculated results of the formation energy under different atomic chemical potential limits indicate that the compensation between As_{Te} and As_{Cd} only occurs for CdTe under Te-rich limit, and occurs for $x=0.5$ and 0.75 under Hg-rich limit. The difference of the formation energies between the As_{cation} and As_{anion} is minimized under cation-rich limit, which is beneficial for the p-type activation of arsenic-doped MCT. Moreover, the calculated transition energy levels indicate that the levels become deeper as the mole fraction becomes larger for both As_{cation} and As_{anion} cases.

IV. CONCLUSION

Using the first-principles method, the structural and bonding mechanisms of *in situ* arsenic impurity in $Hg_{1-x}Cd_xTe$ have been studied. The impurity maintains a relative strong bonding with the host atom both in As_{anion} and As_{cation} cases. The strong bonding mechanism between arsenic and host atom in $Hg_{1-x}Cd_xTe$ can explain its stability of doping behavior. The computed formation energy supports the broadly adopted experimental annealing process, low temperature Hg-saturated annealing process, which minimizes the difference of the formation energy of As_{anion} and As_{cation}. The minimization is beneficial for the atomic transfer during the annealing process. Meanwhile, the nearly linear relationship between the formation energy, both for As_{anion} and As_{cation}, and the mole fraction is shown in the present paper. The transition energy levels for both As_{anion} and As_{cation} agree well with the experimental results. In addition, the present work shows that the compensation effect occurs for CdTe under Te-saturated condition and for 0.5 and 0.75 under Hg-saturated condition.

ACKNOWLEDGMENTS

This work is supported in part by the Scientific Research Fund of Hunan Provincial Education Department (No. 06B092), the National Natural Science Foundation of China (No. 60476040, No. 60576068, No. 10525211, and No. 50561060), and the computational support from Shanghai Supercomputer Center.

*lzsun@xtu.edu.cn
†xschen@mail.sitp.ac.cn
‡luwei@mail.sitp.ac.cn

[1] R. M. Park, M. B. Troffer, C. M. Rouleau, J. M. DePuydt, and M. A. Haase, Appl. Phys. Lett. **57**, 2127 (1990).
[2] M. A. Haase, J. Qiu, J. M. DePuydt, and H. Cheng, Appl. Phys. Lett. **59**, 1272 (1991).
[3] C. H. Park, S. B. Zhang, and Su-Huai Wei, Phys. Rev. B **66**, 073202 (2002).
[4] S. Sivananthan, P. S. Wijewarnasuriya, and J. P. Faurie, Proc. SPIE **2554**, 55 (1995).
[5] D. J. Chadi and K. J. Chang, Phys. Rev. Lett. **61**, 873 (1988).
[6] D. J. Chadi, Phys. Rev. B **59**, 15181 (1999).
[7] Su-Huai Wei and S. B. Zhang, Phys. Rev. B **66**, 155211 (2002).
[8] Sukit Limpijumnong, S. B. Zhang, Su-Huai Wei, and C. H. Park, Phys. Rev. Lett. **92**, 155504 (2004).
[9] H. R. Vydyanath, R. C. Abbott, and D. A. Nelson, J. Appl. Phys. **54**, 1323 (1983).
[10] H. R. Vydyanath, J. A. Ellsworth, and C. M. Devaney, J. Electron. Mater. **16**, 13 (1987).
[11] X. H. Shi, S. Rujirawat, R. Ashokan, C. H. Grein, and S. Sivananthan, Appl. Phys. Lett. **73**, 638 (1998).
[12] C. H. Grein, J. W. Garland, S. Sivananthan, P. S. Wijewarnasuriya, F. Aqariden, and M. Fuchs, J. Electron. Mater. **28**, 789 (1999).
[13] S. Sivananthan, P. S. Wijewarnauriya, F. Awariden, H. R. Vydyanath, M. Zandian, D. D. Edwall, and J. M. Arias, J. Electron. Mater. **26**, 621 (1997).
[14] B. D. Edwall, J.-S. Chen, and L. O. Bubulac, J. Vac. Sci. Technol. B **9**, 1691 (1990).
[15] M. A. Berding and A. Sher, Appl. Phys. Lett. **74**, 685 (1999).
[16] T. C. Harman, J. Electron. Mater. **8**, 191 (1989).
[17] H. R. Vydyanath, Semicond. Sci. Technol. **5**, S213 (1990).
[18] M. A. Berding, A. Sher, M. Van Schilfgaarde, A. C. Chen, and J. Arias, J. Electron. Mater. **27**, 605 (1998).
[19] J. W. Garland, C. H. Grein, B. Yang, P. S. Wijewarnasuriya, F. Aqariden, and S. Sivananthan, Appl. Phys. Lett. **74**, 1975 (1999).
[20] M. Zandian, A. C. Chen, D. D. Edwall, J. G. Pasko, and J. M. Arias, Appl. Phys. Lett. **71**, 2815 (1997).
[21] P. S. Wijewarnasuriya and S. Sivananthan, Appl. Phys. Lett. **72**, 1694 (1998).
[22] L. Z. Sun, X. S. Chen, Y. L. Sun, X. H. Zhou, Zh. J. Quan, He Duan, and Wei Lu, Phys. Rev. B **71**, 193203 (2005).
[23] P. Hohenberg and W. Kohn, Phys. Rev. **136**, B864 (1964); W. Kohn and L. J. Sham, *ibid.* **140**, A1133 (1965).
[24] P. Blaha, K. Schwarz, G. K. H. Madsen, D. Kvasnicka, and J. Luitz, *WIEN2K, An augmented plane wave plus local orbitals program for calculating crystal properties* (Vienna University of Technology, Vienna, Austria, 2001).
[25] J. P. Perdew, K. Burke, and M. Ernzerhof, Phys. Rev. Lett. **77**, 3865 (1996).
[26] R. Yu, D. Singh, and H. Krakauer, Phys. Rev. B **43**, 6411 (1991).
[27] B. Kohler, S. Wilke, M. Scheffler, R. Kouba, and C. Ambrosch-Draxl, Comput. Phys. Commun. **94**, 31 (1996).
[28] G. Kresse and J. Furthmuller, Phys. Rev. B **54**, 11169 (1996).
[29] G. Kresse and J. Furthmuller, Comput. Mater. Sci. **6**, 15 (1996).
[30] D. Vanderbilt, Phys. Rev. B **32**, 8412 (1985).
[31] S. B. Zhang and J. E. Northrup, Phys. Rev. Lett. **67**, 2339 (1991).
[32] J. Lento, J.-L. Mozos, and R. M. Nieminen, J. Phys.: Condens. Matter **14**, 2637 (2002).
[33] Su-Huai Wei and Alex Zunger, Phys. Rev. B **37**, 8958 (1988).
[34] M. Boukerche, P. S. Wijewarnasuriya, S. Sivananthan, I. K. Sou, Y. J. Kim, K. K. Mahavadi, and J. P. Faurie, J. Vac. Sci. Technol. A **6**, 2830 (1988).
[35] L. Z. Sun, Xiaoshuang Chen, Y. L. Sun, X. H. Zhou, Zh. J. Quan, He Duan, and Wei Lu, Phys. Rev. B **73**, 195206 (2006).
[36] P. Boieriu, C. H. Grein, H. H. Jung, J. Garland, and V. Nathan, Appl. Phys. Lett. **86**, 212106 (2005).
[37] S. K. Ghandhi, N. R. Taskar, and I. B. Bhat, Appl. Phys. Lett. **50**, 900 (1987).
[38] L. M. Arias, S. H. Shin, D. E. Cooper, M. Zandian, J. G. Pasko, E. R. Gertner, R. E. DeWames, and J. Singh, J. Vac. Sci. Technol. A **8**, 1025 (1990).
[39] B. Yang, F. Aqariden, C. H. Grein, A. Jandaska, T. S. Lee, A. Nemani, S. Rujirawat, X. H. Shi, M. Sumstine, S. Velicu, and S. Sivananthan, J. Vac. Sci. Technol. B **17**, 1205 (1999).
[40] R. L. Harper, Jr., S. Hwang, N. C. Giles, J. F. Schetzina, D. L. Dreifus, and T. H. Myers, Appl. Phys. Lett. **54**, 170 (1989).